12th International Symposium on Turbulence and Shear Flow Phenomena (TSFP12)
Osaka, Japan (Online), July 19-22, 2022

MODIFICATION OF TAYLOR-COUETTE TURBULENCE IN AN ASYMPTOTIC ULTIMATE REGIME BY THE VISCOELASTICITY OF DILUTE SURFACTANT SOLUTION

Yasufumi Horimoto
Faculty of Engineering
Hokkaido University
060-8628, N13 W8, Sapporo, Hokkaido, Japan
horimoto@eng.hokudai.ac.jp

Taisei Hayama
Graduate School of Science and Technology
Tokyo University of Science

Homare Okuyama
Graduate school of Engineering
Hokkaido University

ABSTRACT

We experimentally investigate the modification of the wall frictional drag and mean flow structures in high Reynolds-number Taylor-Couette turbulence due to the viscoelasticity of a dilute surfactant solution. The examined turbulence is in an asymptotic ultimate regime realized by utilizing a very large facility with co- and counter-rotation of the inner and outer cylinders. We experimentally observe the drag reduction for the counter-rotation cases in a higher Reynolds number regime for the first time while, for the co-rotation, a remarkable drag enhancement as reported by recent numerical studies for the pure inner cylinder rotation [Liu & Khomami, *Phys. Rev. Lett.*, (2013); Song et al., *J. Fluid Mech.*, (2019)]. This drag modification is well understood by defining the Reynolds number based on the bulk shear rate and the viscous timescale, which suggests the the bulk shear rate normalized by the relaxation time of the viscoelasticity (i.e. the Weissenberg number) is an important parameter of the drag modification. For the mean flow structure, we find a non-monotonic profile of azimuthal velocity and a constant angular velocity region (i.e. quasi solid-body rotational flow) in a bulk region. The angular velocity also shows a clear correlation with the drag modification.

INTRODUCTION

Taylor-Couette flow, flow between two concentric cylinder independently rotating, is a one of fundamental flow systems. Utilizing this flow, one can study the dynamics of fluid flow including flow instability, turbulence transition and fully developed turbulence [see a famous flow diagram in Andereck et al. (1986)]. This flow is controlled only by two dimensionless parameters, namely the Reynolds numbers

$$\mathrm{Re}_i = \frac{r_i \omega_i d}{\nu} \quad \text{and} \quad \mathrm{Re}_o = \frac{r_o \omega_o d}{\nu} \tag{1}$$

based on the rotations of the flow for fixed geometrical parameters, the radius ratio $\eta = r_i/r_o$ and the aspect ratio $\Gamma = L/d$ (L is the height of the cylinders). Here, r_i (r_o) and ω_i (ω_o) are the radius and angular velocity of the inner (outer) cylinder, and ν is the kinematic viscosity of the fluid. $d = r_o - r_i$ is the width of the gap between the cylinders. This is an great advantage from an experimental view point because controlling the rotations by motors is easy.

In recent years, quite high Reynolds-number Taylor-Couette turbulence has been investigated by experimentally and numerically where flow has an analogy of turbulent Rayleigh-Bénard convection with a high Rayleigh number with respect to the angular momentum transport [see a recent review by Grossmann et al. (2016) and references therein]. That is, a power law

$$\mathrm{Nu}_\omega \sim \mathrm{Ta}^\beta \tag{2}$$

holds in the angular momentum transport (Eckhardt et al., 2007). Here, Ta is the Taylor number

$$\begin{aligned}\mathrm{Ta} &= \frac{1}{4}\left(\frac{1+\eta}{2\sqrt{\eta}}\right)^4 \frac{(r_o+r_i)^2(\omega_i-\omega_o)^2 d^2}{\nu^2} \\ &= \frac{(1+\eta)^6}{64\eta^4}(\mathrm{Re}_i - \eta \mathrm{Re}_o)^2\end{aligned} \tag{3}$$

and Nu_ω is the angular Nusselt number

$$\mathrm{Nu} = \frac{J^\omega}{J^\omega_{\mathrm{lam}}} \quad \left(J^\omega_{\mathrm{lam}} = 2\nu r_i^2 r_o^2 \frac{\omega_i - \omega_o}{r_o^2 - r_i^2}\right) \tag{4}$$

respectively. $J^\omega = T/2\pi\rho L$ is the angular velocity current across the gap between the cylinders and J^ω_{lam} is its laminar value (ρ: the density of the fluid). The regime where the scaling (2) holds is called an asymptotic ultimate regime. Typically, it appears for a sufficiently high Taylor-number regime, $\mathrm{Ta} \gtrsim 10^9$ (Grossmann et al., 2016). Incidentally, while β is theoretically predicted to be 1/2 as well as turbulent Rayleigh-Bénard convection, it has been shown that $\beta \approx 0.39$ due to the logarithmic correction from many previous studies (Kraichnan, 1962; Doering & Gibbson, 1995; Eckhardt et al., 2007).

In this study, we report the impact of the viscoelastic property of the fluid on Taylor-Couette turbulence in the ultimate regime. More concretely, we experimentally investigate the modification of the frictional drag and flow structure by the addition of a small amount of surfactant to turbulence of water. It is well known that dilute surfactant solution has remarkable viscoelasticity and show large drag reduction compared with turbulence of water due to the suppression of small-scale turbulent eddies (Zakin et al., 1998; Li et al., 2012). However, although this drag reducing effect is very attractive in terms of fluid tranport, turbulence of a viscoelastic fluid is hard to understand because of its peculiar phenomena (Lumley, 1969, 1973;Tabor & de Gennes, 1986; White & Mungal, 2008; Xi, 2019). Hence, researches to elucidate the physical mechanism of the drag reduction has widely conducted for fundamental flow systems such as pipe flow, channel flow, boundary layer, etc. In this context, Taylor-Couette flow is a good candidate because this closed flow system is useful to sustain turbulence generated by strong shear and the wall frictional drag can be directly assessed from torque on the cylinders.

Nevertheless, a little suprisingly, previous studies of turbulent Taylor-Couette flow of viscoelastic flows is limited for relatively low Reynolds number where flow instability and early transitions to turbulence are concerned (e.g. Larson et al., 1990; Avgousti & Beris, 1993; Thomas et al., 2009; Dutcher & Muller, 2013). What is worse, direct numerical simulations (DNS) for $\mathrm{Re}_i = O(10^3)$ and $\mathrm{Re}_o = 0$ shows that the viscoelasticity triggered a pronounced *drag enhancement* rather than drag reduction (Liu & Khomami, 2013; Song et al., 2019). Note that their DNS did not reach the ultimate regime [see Eq. (3)]. In other words, the modification of Taylor-Couette turbulence in the ultimate regimes by the viscoelasticity has not been revealed yet.

In the present study, for the first time, we conducted a series of expriments both for co- and counter-rotation of the cylinders to answer the following question by utilizing a large experimental facility: can the drag reduction occur in the ultimate turbulence of Taylor-Couette flow? We also shows the modification of the flow structure obtained by mesurements of velocity field and discuss the modifications of the ability of angular momentum transport.

EXPERIMENTAL SETUP & METHOD

We use a quite large Taylor-Couette facility to sustain very high Reynolds-number turbulence. It consists of two cylinders independently rotated by stepper motors. The radius and height of the inner cylinder are 150 mm and 990 mm while those of the outer cylinder are 205 mm and 1014 mm, respectively. Thus, the radius ratio and the aspect ratio of the facility are $\eta = 0.732$ and $\Gamma = 18$. The outer cylinder and its top surface are made of acrylic resin for fluid visualization and velocity measurement (explained below).The end surfaces of each cylinder rotate together with the cylinders.

By using a torquemeter set on the shaft of the inner cylinder, the measured torque T on the inner cylinder can be converted into the wall shear stress. Based on this, we estimate the frictional drag by the drag coefficient defined as

$$C_f = \frac{\langle T \rangle_t}{\pi\rho(r_i\omega_i - r_o\omega_o)^2 r_i^2 L}. \tag{5}$$

Here, the bracket $\langle\cdot\rangle$ represents average with respect to the variable on its subscript. We also estimate the angular Nusselt number Nu_ω through $\langle T \rangle_t$ by using $J^\omega = T/(2\pi\rho L)$ to examine the angular momentum transport.

As mentioned above, the outer cylinder and its top surface are made of transparent acrylic resin for flow visualization. To discuss the statistics in turbulent flow, we measure the turbulent field by particle tracking velocimetry (PTV) with the nearest neighbour algorithm. As a tracer particles for PTV, we use silver-coated hollow glass beads (10 µm diameter). A planer laser sheet is in the plane at mid-height of the inner cylinder and a high speed camera above the facility records the motion of the tracer particles visualized by the laser sheet.

We examine a dilute aqueous solution of a cationic surfactant, cetyltrimethylammonium chloride (CTAC. 320.00 g/mol) as a viscoelastic fluid as well as water as a Newtonian fluid. With counterions to reduce the charge on the surface of surfactant micellar structures, the structure can grow and the CTAC solution shows remarkable viscoelasticity due to the existent of very large micellar network structure (Li et al., 2012). As the counterion, we use sodium salicylate (NaSal. 160.11 g/mol). The mass concentrations of CTAC and NaSal are both 100 ppm: the molar ratio of NaSal to CTAC is 2 where the micellar networks are stably exist in the solution. In this study, we estimate the physical quantities of the CTAC solution by those of water at the same temperature because measurements of them are quite difficult for such dilute solution.

RESULTS & DISCUSSION

Drag Modification

In this study, we the rotational condition of the cylinders by using the angular velocity ratio defined as

$$a = -\frac{\omega_o}{\omega_i}. \tag{6}$$

Note that $a < 0$ and $a > 0$ respectively represent the co- and counter-rotation of the cylinder. Fig. 1 shows examples of the torque measurement; the wall frictional eoefficient C_f as a function of the inner Reynolds number Re_i for $a = -0.33$, 0, and 0.33. It is clear that while the drag enhancement occur for $a = -0.33$, 0 [Fig. 1(a,b)], we can observe the specific switch of the drag modification from the enhancement to the reduction for $a = 0.33$ [Fig. 1(c)]. That is, the drag enhancement occurs for a sufficiently high Re_i-region ($\mathrm{Re}_i \gtrsim 4 \times 10^4$).

Here, it is worth mentioning that Fig. 1 shows an answer to the question in the introduction. More concretely, the drag reduction in turbulent Taylor-Couette flow by the viscosity can be expected for a high Reynolds-number regime. To confirm this, we conduct the torque measurement for a wide range of a; $-0.5 \le a \le 0.5$. The results are summarized in Fig. 2(a). In this figure, the drag modification is quantified by the drag reduction fraction

$$\mathrm{DR} = \frac{C_{f,\mathrm{w}} - C_{f,\mathrm{s}}}{C_{f,\mathrm{w}}} \times 100. \tag{7}$$

Here, $C_{f,\mathrm{w}}$ and $C_{f,\mathrm{s}}$ are the drag coefficient for water and the srufactant (CTAC) solution, respectively.

First of all, from Fig. 2(a), we notice that DR is larger for larger a, and the clear drag reduction is observed for the cases of counter rotation ($a > 0$) in a higher Re_i-regime up to 50%. On the other hands, for $a \le 0$, only drag enhancement (DR < 0) appears and it is more remarkable than the

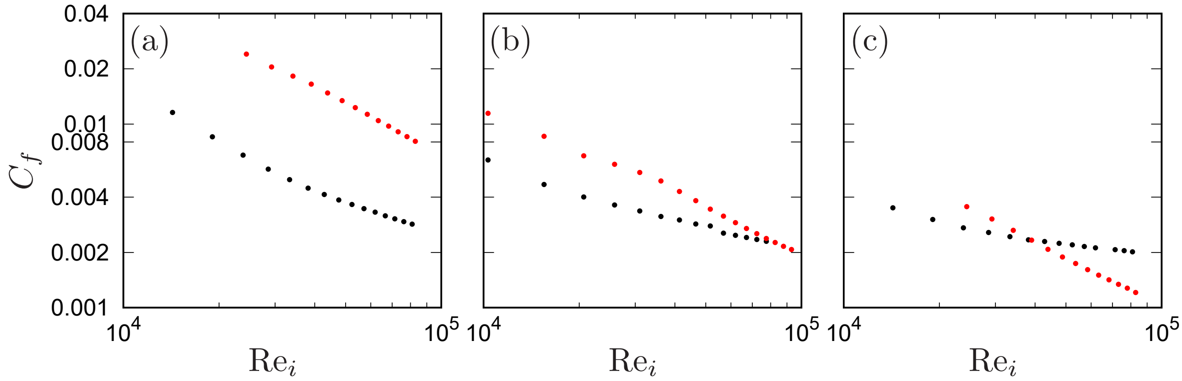

Figure 1. Wall frictional coefficient C_f as a function of the inner cylinder Reynolds number Re_i for (a) co-rotation ($a=-0.33$), (b) pure inner cylinder rotation ($a=0$), and (c) counter-rotation ($a=0.33$). Black and red dots represent the cases for water and surfactant solution (100 ppm), respectively.

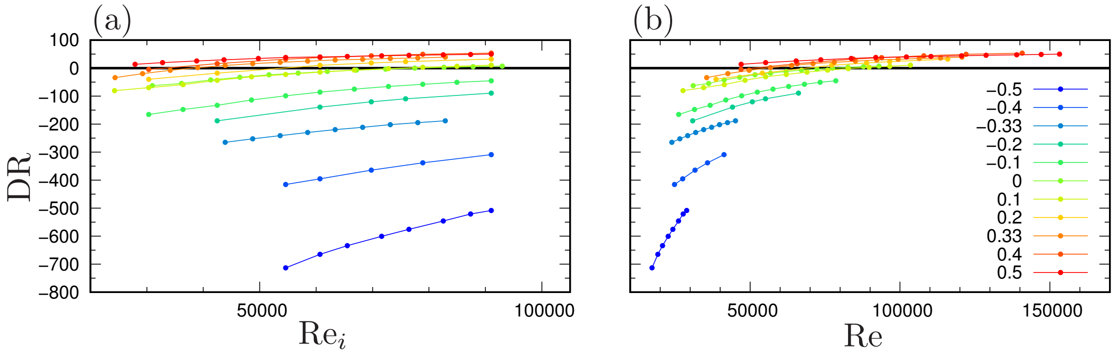

Figure 2. Drag reduction ratio DR as a fuction of (a) Re_i and (b) Re for $-0.5 \leq a \leq 0.5$. The colors correspond the values of a as shown in (b).

above drag reduction. However, the Re_i-dependence that DR increases with Re_i is common for all value of a. Hence, even for co-rotation ($a<0$), the drag reduction can be expected in a much more high Re_i-regime.

Next, we consider what parameter is suitable for the understanding of the drag modification. Recalling the definition (6) of a, we notice that a characteristic shear rate $\dot{\gamma} = (r_i\omega_i - r_o\omega_o)/d$ is higher for larger a. To make it clear, we define another Reynolds number as

$$\mathrm{Re} = \frac{(R_i\omega_i - R_o\omega_o)d}{\nu} = \mathrm{Re}_i - \mathrm{Re}_o. \qquad (8)$$

Note that Re^{-1} indicates the ratio of a time scale of the flow $\dot{\gamma}^{-1}$ to the viscous time scale d^2/ν. We replot DR as a function of Re in Fig. 2(b). It is obvious that DR seems to be well collapsed on a curve as an envelop. Hence, this shows that the flow time scale $\dot{\gamma}^{-1}$ is an important parameter for the drag modification in viscoelastic Taylor-Couette turbulence. This results is reasonable by noting that a dilute surfactant solution has single (or sometimes a few) relaxation time τ of the viscoelasticity (Zakin et al., 1998; Li et al., 2012). That is, the Reynolds number Re_c, which is $\mathrm{Re}_c \in [5000, 7000]$ for our experimental setup, where the drag enhancement turns to the drag modification is given a function of the Weissenberg number $\mathrm{We} = \tau\dot{\gamma}$.

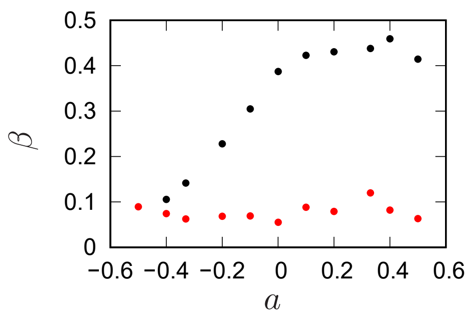

Figure 3. Scaling index β in the scaling law (2) of angular momentum transfer as a function of the angular velocity ratio a. Black and red dots represent the cases for water and surfactant solution (100 ppm), respectively.

Angular Momentum Transport

To discuss the modification of angular momentum transport, we show the scaling exponent β in Eq. (2) for the various values of a. The examined Reynolds-number regime shown above corresponds to $\mathrm{Ta} \gtrsim 10^9$, which is the ultimate regimes, and we confirm the scaling law (2) indeed holds both for water and the CTAC solution (figures are omitted).

For water, β reaches around 0.4 as well known by many previous studies for $a \gtrsim 0$ (Grossmann et al, 2016). Incidentally, accoding to the discussion of Gils et al. (2012), β has the maximum value around the bisection line between two neutral lines in Re_i–Re_o space, the pure outer cylinder rotation

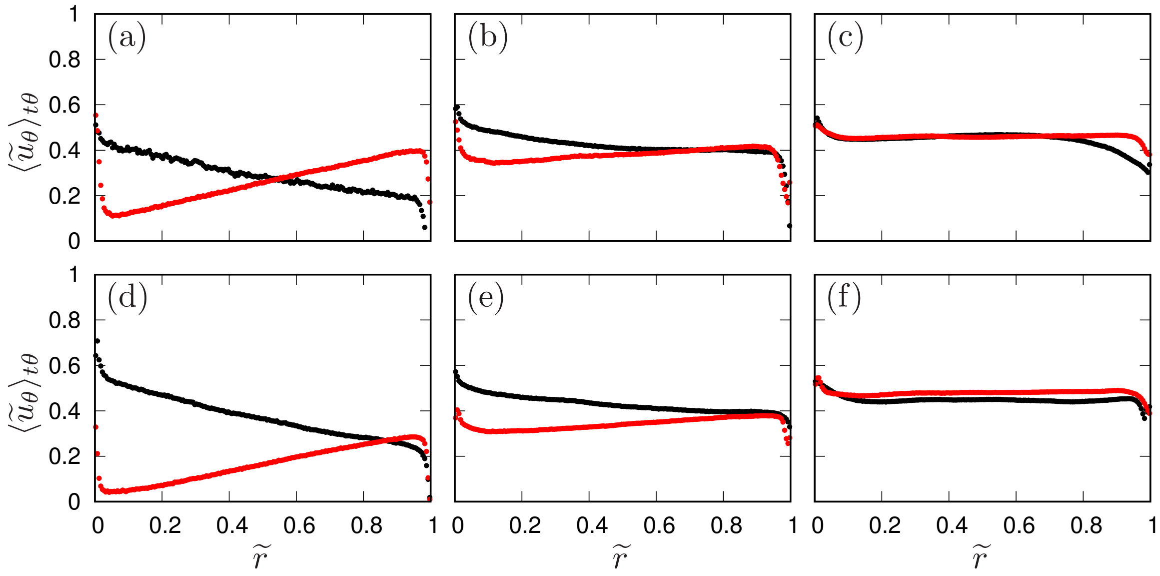

Figure 4. Radial profile of mean azimuthal velocity profile $\langle \widetilde{u}_\theta \rangle_{t\theta}$ for (a-c) $\mathrm{Re}_i = 4.3 \times 10^4$ and (d-f) $\mathrm{Re}_i = 7.0 \times 10^4$. Black and red dots represent the cases for Newtonian fluid (water) and viscoelastic fluid (the CTAC solution), respectively. (a,d) Counter-rotation ($a = 0.33$), (b,e) pure inner cylinder rotation ($a = 0$), and (c,f) co-rotation ($a = -0.33$).

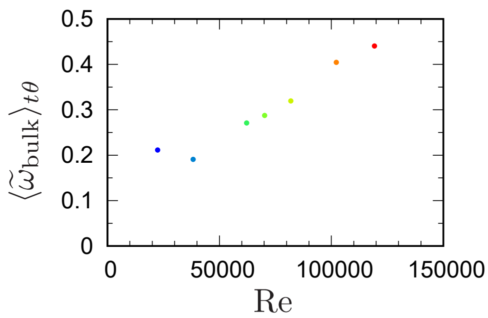

Figure 5. Re-dependence of the angular velocity $\langle \widetilde{\omega}_{\mathrm{bulk}} \rangle_{t\theta}$ in the quasi SBR region for $a = \pm 0.5$, ± 0.33, ± 0.1, and 0. Colors are the same as those shown in Fig. 2.

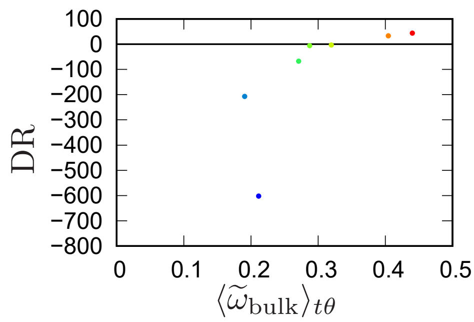

Figure 6. Relation between the angular velocity $\langle \widetilde{\omega}_{\mathrm{bulk}} \rangle_{t\theta}$ in the quasi SBR region and the drag reduction rate DR for $a = \pm 0.5$, ± 0.33, ± 0.1, and 0. $\mathrm{Re}_i = 7.1 \times 10^4$ only for $a = \pm 0.5$ and $\mathrm{Re}_i = 7.0 \times 10^4$ for the others. Colors are the same as those shown in Fig. 2.

($a \to \infty$) and the Rayleigh criterion ($a = -\eta^2$) for the centrifugal instability. The bisection line corresponds to a value a_{bis} of the angular velocity ratio. For the present setup ($\eta = 0.732$), $a_{\mathrm{bis}} = 0.371$, which is show that the result for water is reasonable for the previous study.

On the other hand, for the CTAC solution, β show a quite different trend. That is, β is drastically reduced for counter-rotation ($a > 0$) and keep around 0.1 over the examined range of a. This shows that the angular momentum transport is also reduced by the viscoelasticity as well as the wall frictional drag (shown in Fig. 2).

Mean Velocity Modification

Finally, we discuss the modification of mean flow structure. Figure 4 shows the radial profile of mean azimuthal velocity $\langle u_\theta \rangle_{t\theta}$. Here, the velocity and radial position is normalized as

$$\widetilde{r} = \frac{r - r_o}{d} \quad \text{and} \quad \widetilde{u}_\theta = \frac{u_\theta - r_o\omega_o}{r_i\omega_i - r_o\omega_o}. \tag{9}$$

We notice a remarkable modification of the profiles for the drag enhancement cases ($a = -0.33$ and 0). That is, quite surprisingly, the velocity gradient is nonmonotonic; it turns positive in a bulk region while it is negative near the wall. Furthermore, in the bulk region, the velocity profile seems to be linear, which implies that there is a flow structure rotating as if it is solid body between the cylinders. We call this the quasi solid body rotational (SBR) region. It is worth mentioning that although the previous DNS showing the drag enhancement in the viscoelastic turbulent Taylor-Couette flow reported a similar nonmonotonic profile for $\mathrm{Re}_i = 5000$ (Liu % Khomami 2013) and $\mathrm{Re}_i = 3000$ (Song et al. 2019), they did not show such quasi SBR region probably because the Reynolds number is not so high and they treat the pure inner cylinder rotation.

From the results of PTV, we calculate the profiles of the angular velocity by using $\langle \omega \rangle_{t\theta} = \langle u_\theta \rangle_{t\theta} / r$ and normalizing it as

$$\widetilde{\omega}_\theta = \frac{\langle \omega \rangle_{t\theta} - \omega_o}{\omega_i - \omega_o}. \tag{10}$$

We define the angular velocity $\langle \widetilde{\omega}_{\rm bulk} \rangle_{t\theta}$ of the bulk region as the average in $0.2 \leq \widetilde{r} \leq 0.8$. Figure 5 show the Re-dependence of the angular velocity $\langle \widetilde{\omega}_{\rm bulk} \rangle_{t\theta}$ in the quasi SBR regeion for $a = \pm 0.5$, ± 0.33, ± 0.1, and 0 [colors are the same as shown in Fig. (2)]. Due to the resolution of the angular velocity on the present set up, the inner cylinder Reynolds number for $a = \pm 0.5$ ($\mathrm{Re}_i = 7.1 \times 10^4$) is slightly different from the others ($\mathrm{Re}_i = 7.0 \times 10^4$).

It is obvious that there is a positive correlation between Re and $\langle \widetilde{\omega}_{\rm bulk} \rangle_{t\theta}$. We can understand this result by recalling that the definition of Re: a higher Re means larger shear rate $\dot{\gamma}$ in a bulk region. That is, the viscoelasticity has a larger effect and the angular velocity in quasi SBR region becomes larger. Here this result might be confusing in the comparison with that in Fig. 4 but notice that the difference of the normalization of velocity [Eq. (9)] and angular velocity [Eq. (10)]. Furthermore, as expected the Re-dependence of DR [Fig. 2(b)] and $\langle \widetilde{\omega}_{\rm bulk} \rangle_{t\theta}$ (Fig. 5), DR show the positive correlation with $\langle \widetilde{\omega}_{\rm bulk} \rangle_{t\theta}$ as shown in Fig. 6 implying that the quasi SBR region is important for the drag modification [colors are the same as shown in Fig. (2)].

CONCLUSION

To elucidate the modification of high Reynolds-number Taylor-Couette turbulence by the viscoelasticy of a dilute surfactant (CTAC) solution, we investigate the wall fcirtion and turbulent velocity field by utilizing a quite large experimental facility. We examined the turbulence both for the co-cotation ($a < 0$) and counter-rotation ($a > 0$) of the two cylinders.

We ovserve the drag reduction up to DR $= 50\%$ for the counter-rotation for the first time while the drag enhancement DR < 0 for the co-rotation and the pure inner cylinder rotation ($a = 0$) as well as the previous DNS (Liu & Khomami, 2013; Song et al., 2019) (Fig. 2). This drag modification can be unifiedly represented by a Reynolds number Re indicating the shear on the bulk region [Eq. (8)]. The viscoelasticity of the CTAC solution also modifies the angular momentum transport in Taylor-Couette turbulence in the ultimate regime where the scaling law (2) holds. The scaling exponent is reduced and almost the same even for the counter-rotation as that for the co-rotation (Fig. 3).

Concerning the mean flow structures, a nonmonotonic velocity profile and the quasi solid body rotational region in a bulk appear for the CTAC solution as shown in Fig. 4. Such quasi SBR regime seems to be exist for a sufficiently higher Reynold-number regime. The magnitude of the angular velocity of the quasi SBR region is larger for higher Re and has a positive correlation with DR, which implys that the occurrence of this quasi SBR region is important to discuss the drag reduction in Taylor-Couette turbulence in the ultimate regime.

In the conference, we will present the more detailed results about the flow structures and discuss the sustainaning mechanism of the quasi SBR region by showing the results for other Reynolds-number regimes.

ACKNOWLEDGEMENT

This study was partially supported by JSPS Trant-in-Aid for Early-Careere Scientists (19K14893).

REFERENCES

Andereck, C. D., Liu, S. S. and Swinney, H. L., 1986, ”Flow regimes in a circular Couette system with independently rotating cylinders”, Journal of Fluid Mechanics, Vol. 164, pp. 155-183.

Doering, C. R., and Gibbon, J. D., 1995, ”Applied Analysis of the Navier-Stokes Equations”, Cambridge Univ. Press, Cambridge.

Dutcher, C. S., and Muller, S. J., 2013, ”Effects of moderate elasticity on the stability of co- and counter-rotating Taylor-Couette flows”, Journal of Rheology, Vol. 57, pp. 791-812.

Eckhardt, B., Grossmann, S., and Lohse, D., 2007, ”Torque scaling in turbulent Taylor-Couette flow between independently rotating cylinders”, Journal of Fluid Mechanics, Vol. 581, pp. 221-250.

Van Gils, D. P. M., Huisman, S. G., Grossmann, S., Sun, C., and Lohse, D., 2012, ”Optimal Taylor–Couette turbulence”, Journal of Fluid Mechanics, Vol. 706, pp. 118-149.

Grossmann, S., Lohse, D., and Sun, C., 2016, ”High–Reynolds number Taylor-Couette turbulence”, Annual Review of Fluid Mechanics, Vol. 48, pp. 53-80.

Kraichnan, R. H., 1962, ”Turbulent thermal convection at arbitrary Prandtl number”, Physics of Fluids, Vol. 5, pp. 1374-1389.

Li, F.-C., Yu, B., Wei, J.-J., and Kawaguchi, Y., 2012, ”Turbulent Drag Reduction by Surfactant Additives”, Wiley, New York.

Liu, N., and Khomami, B., 2013, ”Polymer-induced drag enhancement in turbulent Taylor-Couette flows: direct numerical simulations and mechanistic insight”, Physical Review Letters, Vol. 111, 114501.

Lumley, J. L., 1969, ”Drag reduction by additives”, Annual Review Fluid Mechanics, Vol. 1, pp. 367-384.

Lumley, J. L., 1973, ”Drag reduction in turbulent flow by polymer additives”, Journal of Polymer Science Macromolcular Reviews, Vol. 7, pp. 263-290.

Larson, R. G., Shaqfeh, E. S. G., and Muller, S. J., 1990, ”A purely elastic instability in Taylor-Couette flow”, Journal of Fluid Mechanics, Vol. 218, pp. 573-600.

Avgousti, M. and Beris, A. N., 1993, ”Non-axisymmetric modes in viscoelastic taylor-couette flow”, Journal of Non-Newtonian Fluid Mechanics, Vol. 50, pp. 225-251.

Song, J., Teng, H., Liu, N., Ding, H., Lu, X., and Khomami, B., 2019, ”The correspondence between drag enhancement and vortical structures in turbulent Taylor–Couette flows with polymer additives: a study of curvature dependence”, Journal of Fluid Mechanics, Vol. 881, pp. 602-616.

Tabor, M., and de Gennes, P. G., 1986, ”A cascade theory of drag reduction”, Europhysics Letters, Vol. 2, pp. 519-522.

Thomas, D. G., Khomami, B., and Sureshkumar, R., 2009, ”Nonlinear dynamics of viscoelastic Taylor-Couette flow: effect of elasticity on pattern selection, molecular conformation and drag”, Journal of Fluid Mechanics, Vol. 620, pp. 353-382.

White, C. M. and Mungal, M. G., 2008, ”Mechanics and prediction of turbulent drag reduction with polymer additives”, Annual Review Fluid Mechanics, Vol. 40, pp. 235-256.

Xi, L., 2019, ”Turbulent drag reduction by polymer additives: fundamentals and recent advances”, Physics of Fluid, Vol. 31, 121302.

Zakin, J. L., Lu, B., and Bewersdorff, H.-W., 1998, ”Surfactant drag reduction”, Reviews in Chemical Engineering, Vol. 14, pp. 253-320.